

LARGE DISPLACEMENT ANALYSIS OF ELASTIC-PLASTIC FRAMES:  
A NUMERICAL AND EXPERIMENTAL STUDY

Severino P. Cavalcanti Marques  
Departamento de Engenharia Estrutural-EES/UFAL  
Campus A. C. Simões, Maceió - AL - Brasil - 57000

Guillermo J. Creus  
Curso de Pós Graduação em Engenharia Civil - UFRGS  
Avenida Osvaldo Aranha, 99 - Porto Alegre - RS - Brasil - 90210

RESUMEN

Es presentado un estudio numérico y experimental de pórticos elastoplásticos. El procedimiento numérico usado es incremental-iterativo y permite la descripción de la respuesta estructural de pórticos espaciales con desplazamientos finitos. Fueron realizados tambien ensayos sobre modelos metálicos planos. Los resultados numéricos y experimentales son comparados.

ABSTRACT

A numerical and experimental study of elastic-plastic frames is presented. The numerical formulation is incremental - iterative and allows the description of the structural behavior of space frames with arbitrarily large displacements. Tests on small scale models of metallic plane frames were performed. Numerical and experimental results are compared.

INTRODUCTION

The use of very slender metal structures and the need to take full advantage of materials strength have increased the importance of geometrical and material nonlinear effects in formulations for structural analysis. Two of the pionner works that used computational resources for the elastic-plastic analysis of space frames were proposed by BRUNETTE[1] and MORRIS[2]. Among the formulations that take into account geometrical and material nonlinear effects we can mention those by ARGYRIS[3] and SHI[4].

In this work we present a numerical and experimental study of elastic-plastic frames with finite displacements. The numerical procedure is incremental-iterative and allows the analysis of space frames in the

pre and post-critical stages, including the situations where displacement increase occurs together with loading decrement, or when decrease of displacements occurs with increasing loads. The kinematics relations[5] allow the manipulation of arbitrarily large displacements associated with small strains. For the numerical solution of the iterative-incremental problem the Work Control Method[6] is employed.

The elastic-plastic behavior of the members is modelled using the plastic hinge concept based on generalized yield criterium. For elements that present one or two plastic hinges in their ends, an elastoplastic stiffness matrix is presented. The expression for this matrix includes a parameter that aims to take into account, approximately, the strain-hardening of the material. The geometrical stiffness matrix is based on semitangential moments[7].

The formulation was implemented into a computational code in FORTRAN language for microcomputers. To check the numerical results, tests on small metallic models were also performed. The results of experimental and numerical examples are presented.

## NUMERICAL FORMULATION

### Assumptions

The numerical procedures are based on following assumptions:

- 1) The displacements are arbitrarily large and the strains are small
- 2) The loads are nodal and change proportionally.
- 3) The material has elastoplastic behavior, perfect or with isotropic hardening.
- 4) The members are straight, prismatic and have doubly symmetric sections.
- 5) The plastification only occurs at the ends of the elements and is concentrated in one section; that is, the plastic hinge concept is adopted.
- 6) The concepts of the associated plasticity are employed.

### Tangent stiffness matrix of the elements

The criterium for plastification of a element cross section, considering isotropic hardening, may be written as

$$\Psi(\{P\}) = k \quad (1)$$

where  $\{P\}$  is the member stress resultants vector and  $k$  is a parameter which depends on plastic displacements.

If  $\{U^e\}$  and  $\{U^p\}$  denote, respectively, the elastic and plastic parts of the displacements  $\{U\}$  of a element, we can write in terms of rates that

$$\{\dot{U}\} = \{\dot{U}^e\} + \{\dot{U}^p\} \quad (2)$$

being

$$\{\dot{U}^e\} = [K_e]^{-1} \{\dot{P}\} \quad \{\dot{U}^p\} = \dot{\lambda}^i \{B\}^i \quad (3)$$

where [Ke] is the elastic stiffness matrix which is the sum of the conventional stiffness matrix[B] with the geometrical stiffness matrix of the element[7].  $\dot{\lambda}$  is a scalar function[9] and  $\{B\}^i = (\partial\psi/\partial\langle P \rangle)^i$  is the gradient vector of  $\psi$ , corresponding to the stress resultants  $\langle P \rangle^i$  at end  $i$  ( $i = 1$  or  $2$ ) of the element.

For an element with one plastic hinge at its end 1, the use of (2) and (3) leads to

$$\langle B \rangle^{iT} \langle \dot{P} \rangle^i = \langle B \rangle^{iT} [K_{11}] \langle \dot{U} \rangle^i - \dot{\lambda}^i \langle B \rangle^{iT} [K_{11}] \langle B \rangle^i + \langle B \rangle^{iT} [K_{12}] \langle \dot{U} \rangle^2 \quad (4)$$

where  $[K_{ij}]$  represents submatrices of order  $6 \times 6$  of [Ke].

Now, if we make  $\langle B \rangle^{iT} \langle \dot{P} \rangle^i = A \dot{\lambda}^i$ , being A the strain-hardening parameter, then

$$\dot{\lambda}^i = \frac{\langle B \rangle^{iT} [K_{11}] \langle \dot{U} \rangle^i}{A + \langle B \rangle^{iT} [K_{11}] \langle B \rangle^i} \quad (5)$$

Using the expressions (2), (3), (4) and (5) we obtain

$$\langle \dot{P} \rangle = [Ke] \left[ [I] - \frac{[B] [B]^T [Ke]}{A + \langle B \rangle^{iT} [K_{11}] \langle B \rangle^i} \right] \langle \dot{U} \rangle \quad (6)$$

where  $[B]^i = [\langle B \rangle \quad \{0\}]$  and [I] is the identity matrix.

The equation (6) shows that

$$[Kep] = [Ke] \left[ [I] - \frac{[B] [B]^T [Ke]}{A + \langle B \rangle^{iT} [K_{11}] \langle B \rangle^i} \right] \quad (7)$$

represents the tangent elastoplastic stiffness matrix of the element.

For an element with a plastic hinge in its end 2, the matrix [Kep] is given by (7), changing the index 1 to 2 and making  $[B] = [\{0\} \langle B \rangle^{2T}]$ .

When the element has two plastic hinges we can show, considering the same strain-hardening parameter for both ends, that

$$[Kep] = [Ke] \left[ [I] - [B][C]^{-1}[B][Ke] \right] \quad (8)$$

where

$$[C] = \begin{bmatrix} A + \langle B \rangle^{iT} [K_{11}] \langle B \rangle^i & \langle B \rangle^{iT} [K_{12}] \langle B \rangle^2 \\ \langle B \rangle^{2T} [K_{21}] \langle B \rangle^i & A + \langle B \rangle^{2T} [K_{22}] \langle B \rangle^2 \end{bmatrix} \quad (9)$$

and

$$[B] = \begin{bmatrix} \langle B \rangle^i & \{0\} \\ \{0\} & \langle B \rangle^2 \end{bmatrix} \quad (10)$$

#### Remarks on the strain-hardening parameter A

Traditionally, the plastic hinge concept was related to limit analysis and thus to perfectly plastic materials. Besides mild steel structures conform fairly well to the perfectly plastic model. On the other hand, modern materials, particularly new steel and aluminium alloys, show a strain hardening that may present an important influence on the structural behavior, particularly with reference to stability, see [10]. Thus, as early as 1966, DAVIES[10] proposed a method to determine collapse loads for plane frames taking hardening into account. In this method was used a empiric formula to compute the hardening parameter.

In fact, the introduction of hardening is not too easy, principally for the tridimensional frame case. Perhaps the simplest procedure that may be used consists in considering the concept of a lumped hardening hinge as a spring with a rotational stiffness. If only the influence of a bending moment is taken into account, this model leads to a value of

$$A = \frac{4}{3} \frac{1}{M_p^2} \frac{\partial M}{\partial \theta_p} \quad (11)$$

where  $M_p$  is the plastification moment of the section and  $\theta_p$  is the rotation in the plastic hinge. The value of  $\partial M / \partial \theta_p$  is obtained from the experimental moment-curvature diagram derived from a bending test by the relation

$$\frac{\partial M}{\partial \theta_p} = \frac{1}{a} \frac{\partial M}{\partial \kappa_p} \quad (12)$$

where  $a$  is the length of the real hinge and  $\kappa_p$  is the curvature of the bar in the neighbourhood of the plastic hinge.

#### Remarks on the numerical formulation

The numerical procedures are based on an incremental-iterative updated Lagrangian formulation which adopts the kinematics relations proposed by DRAN[5] and the Work Control Method presented by YANG[6] for numerical solution.

The Work Control Method uses the following condition to determine the load increments in each incremental step of the analysis: the work performed by the load increments during the first iteration of the step is equal to a pre-determined value  $\Delta W$  and null for the next iterations of the same step. In the present paper,  $\Delta W$  is defined as a fraction (example, 1/10) of the work performed by the yield loading of the structure which is obtained by means of a linear analysis.

During the development of the analysis, the stiffness matrix of each element is updated at the end of each iteration with base on the current nodal coordinates and stress resultants acting on the element ends. When the unbalanced forces vector of the structure obtained at the of an iteration satisfies a certain convergence criterium, the incremental step is terminated and thus a verification whether the stress resultants on the ends of the elements satisfy the

plastification criterium is performed. When this occurs, the elastic stiffness matrices of the elements with plastic hinges are replaced by the corresponding elastoplastic stiffness matrices. Besides this, a verification of desactivation of already existent plastic hinges also must be performed. The desactivation of a plastic hinge is detected with the signal of the scalar function  $\Lambda$ : a negative signal indicates elastic unloading[9].

At the beginning of each step we must compute, using a linear analysis, the minimum increment of loads needed to activate one or more new plastic hinges. Thus, to control the distance between the stress resultant point and the plastification function  $\Psi$ , we impose the condition that the load increment of the first iteration of the step should not be greater than that minimum value.

In the computational code the following approximated plastification criterium for rectangular section was implemented:

$$\Psi = (M_y/M_{uy})^\alpha + (M_z/M_{uz})^\beta = k \quad (13)$$

with  $\alpha = \beta = 2$ ,  $M_{uy} = M_{py} (1 - N_x^2/N_p^2)$  and  $M_{uz} = M_{pz} (1 - N_x^2/N_p^2)$ .

and

$N_x, M_y, M_z$  - normal force and bending moments acting on the section

$N_p, M_{py}, M_{pz}$  - normal force of plastification and bending moments of plastification of the section.

More details on the numerical formulation may be seen in the references [9] and [11].

#### REMARKS ON THE EXPERIMENTAL TESTS

The experiments were performed on small scale models fabricated with an aluminium alloy, whose stress-strain relation was determined in a strain-gages instrumented tension test(Figure 1).

The experiments on the models were made in a steel test frame of cubical shape. Loading was applied through direct weights calibrated to  $\pm 1\%$ . Displacements of a characteristic point of the structure were measured over a three-dimensional reference scale system fixed in the test frame. Measurement of horizontal and vertical displacements could be determined with a  $\pm 0.5$  mm appreciation, that is reasonable for the case of large displacements.

#### EXAMPLES

a) Cantilever beam under concentrated load at the free end

This example is frequently used as a benchmark[12]. For the elastic case the present formulation gives results very close to the analytical solution[12]. To check numerical results of the elastoplastic analysis, tests were performed on cantilever beams fabricated with aluminium alloy, with the geometrical characteristics shown in the Figure 2.

In the numerical solution run without consideration of hardening a

yield stress of 180 MPa was adopted, following the 0.2 % plastic strain criteria. In the numerical solution considering hardening was adopted  $A = 0.005 \text{ N}^{-1} \text{ cm}^{-1}$ . This value was estimated based in the moment - curvature diagram determined in the neighbourhood of the fixed end and obtained from the strains measured with strain gages instalated in the faces of the beam. The real size of the plastic hinge was taken equal to 2 cm.

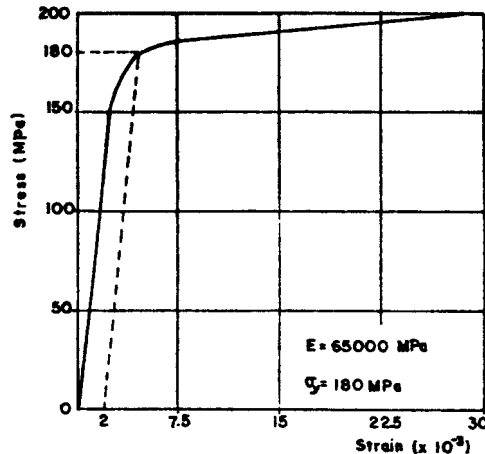


Figure 1. Stress-strain relation for the aluminium alloy

Figure 3 presents a comparison between the experimental results and the numerical solutions in which the cases of perfectly elastoplastic and strain-hardening elastoplastic material were considered. The major differences observed may be explained by following reasons. In the reality, the elastic-plastic transition occurs smoothly, while in the numerical solutions this transition is considered to occur abruptly. Furthermore, the plastic effects are not concentrated in one section, but they occur over a finite length. Figure 3 shows also that due to the strain-hardening effect, the perfectly elastoplastic solution deviates from the experimental results as the plastic deformation increases. On the other hand, the strain-hardening numerical solution is in better agreement with experimental results, as was to be expected.

#### b) Z-Shaped beam

A Z-shaped cantilever beam as shown in Figure 4 has been proposed as a benchmark problem for testing capabilities of codes for nonlinear analysis[13]. This problem was called "Cologne Challenge".

Our numerical analysis used a 10 elements discretization and a perfectly plastic relation with 575 Mpa yield stress. Comparison of numerical and analytical results are shown in Figure 5. ( $v$  = vertical displacement at free end of the beam).

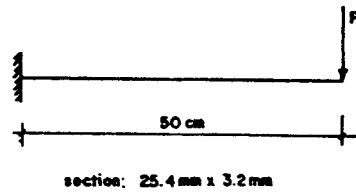


Figure 2. Cantilever beam model

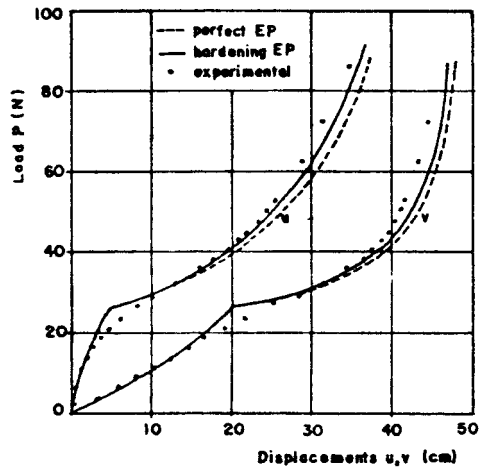


Figure 3. Load - displacements relation of the cantilever beam  
( $u, v$  - horizontal and vertical displacement of the free end)

The Z-shaped beam model of aluminium alloy shown in Figure 6 was studied experimentally and the results obtained are presented together with the numerical solution in Figure 7. The same comments made for the former example are valid for this case.

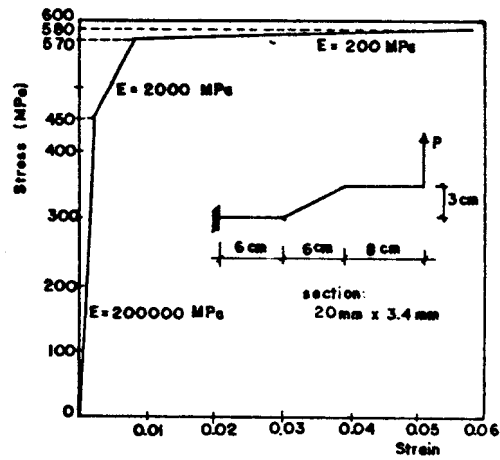


Figure 4. The Cologne Challenge problem

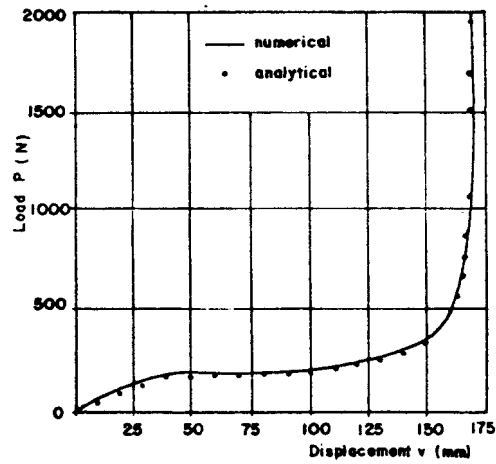


Figure 5. Numerical and analytical solutions of the Cologne Challenge



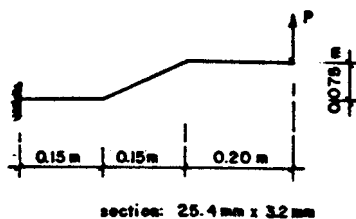


Figure 6. Z-shaped beam model

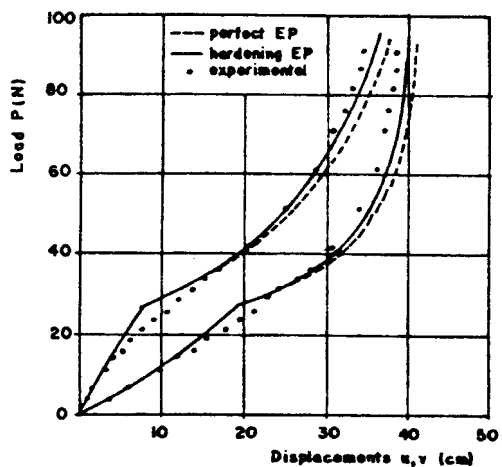


Figure 7. Numerical and experimental results for Z-shaped beam

#### CONCLUSIONS

The numerical formulation described allows the elastoplastic analysis of frames with finite displacements. The isotropic hardening model presented seems to improve the perfectly elastoplastic model. The experimental results for the tested models shown reasonable agreement with the numerical solutions.

#### ACKNOWLEDGEMENTS

The authors are grateful to CAPES and CNPq for the financial support received during the preparation of this work.

REFERENCES

1. Bruinette, K.E. and Fenves, S.J., "A General Formulation of the Elastic-Plastic Analysis of Space Frameworks", International Conference on Space Structures, Univ. of Surrey, 1966.
2. Morris, G. A. and Fenves, S.J., "A General Procedure for the Analysis of Elastic and Plastic Frameworks", SRS No.325, Depart. of Civil Engineering, Univ. of Illinois, Aug., 1967.
3. Argyris, J.H., Boni, B., Hindenlang, U. and Kleiber, M., "Finite Element Analysis of Two- and Three Dimensional Elasto-Plastic Frames The Natural Approach", Computer Methods in Applied Mechanics and Engineering, 35, 1982, pp. 221-245.
4. Shi, G. and Atluri, S.N., "Elasto-Plastic Large Deformation Analysis of Space Frames: a Plastic-Hinge and Stress-Based Explicit Derivation of Tangent Stiffnesses", International Journal for Numerical Methods in Engineering, Vol. 26, 1988, pp. 589-615.
5. Oran, C., "Tangent Stiffness in Space Frames", Journal of the Structural Division, ASCE, Vol. 99, No.ST6, Proc. Paper 9813, June, 1973, pp. 987-1001.
6. Yang, Y.B., "Linear and Nonlinear Analysis of Space Frames with Nonuniform Torsion Using Interactive Computer Graphics", Department of Structural Engineering Report, Cornell University, Number 84-10, June, 1984.
7. Argyris, J.H., Hilpert, O., Malejannakis, G.A. and Scharpf, D.W., "On the Geometrical Stiffness of a Beam in Space - A Consistent V. W. Approach, Computer Methods in Applied Mechanics and Engineering, 20, 1979, pp. 105-131.
8. Gere, J.M. and Weaver Jr, W., "Analysis of Framed Structures", Van Nostrand Reinhold Ltd., New York, 1965.
9. Marques, S.P.C., "Análise Não-Linear Física e Geométrica de Pórticos Espaciais". Dissertação de Mestrado, Curso de Pós-Graduação em Engenharia Civil da UFRGS, 1990.
10. Davies, J.M., "Frame Instability and Strain Hardening Plastic Theory", Journal of the Structural Division, ASCE, Vol.92, No. ST3, June, 1966, pp. 1-15.
11. Marques, S.P.C. e Creus G.J., "Análise Não-Linear Física Geométrica de Pórticos Espaciais". XI Congresso Ibero Latino Americano sobre Métodos Computacionais para Engenharia, 1990.
12. Smith, M., "The NAFEMS Benchmark Tests for Two-Dimensional Thin Beams and Axisymmetric Shells with Geometric Nonlinearity, Benchmark, April, 1990, pp. 13-15.
13. Schwering, W.P.S., "The Cologne Challenge", Finite Element News, Issue No.4, August, 1984.